Crosslinking of Epoxy-Modified Phenol Novolac (EPN) Powder Coatings: Particle Size and Adhesion†

B.D. Pennington, J.C. Grunlan, and M.W. Urban*—The University of Southern Mississippi

These studies were undertaken to examine how particle size of epoxy phenol novolac (EPN) powder coatings may affect adhesion to metal substrates. Particle sizes of 21 and 83 μm diameter were utilized. DSC analysis shows that the activation energies of crosslinking for the 21 μm particle size is 41 kJ/mol and 58 kJ/mol for 83 μm particle size which is attributed to the effect of particle size, and time-temperature-particle size (TTPS) parameters are used to describe powder-liquid-solid film transformation process. Although, the TTSP term represents a combination of intrinsic and extrinsic properties. We believe that this is the TTPS term that adequately describes the processes in which, in order for crosslinking reactions to occur, particles must initiate the flow. Quantitative attenuated total reflectance (ATR) Fourier transform infrared (FTIR) spectroscopic analysis was used to follow crosslinking processes by monitoring the decrease of oxirane concentration, and showed that for thermal cure at 185°C for 20 min, the oxirane concentration decreases at a similar rate for 21 μm and 83 μm particle sizes. The results of pull-off adhesion measurements from an Al substrate show that when the 21 μm particle size is crosslinked for 10 min at 110, 140, and 170°C, adhesion is consistently higher than for the same coating system at 83 μm particle size. This difference is attributed to the finite time required for powder particles to reach a proper melt viscosity, followed by reactions of functional groups leading to crosslinking. Extended cure times to 120 min for the 83 μm particle resulted in adhesion similar to the 21 μm particle size.

INTRODUCTION

Epoxide functionalities are commonly incorporated into coating formulations because they promote adhesion of coatings to a wide variety of substrates, including metals and glasses.[1-3] Reactions of epichlorohydrin (ECH) with hydroxyl, carboxyl, and amino functional groups will lead to the formation of epoxide functionalities, which are capable of withstanding higher shear stresses, but exhibit weaker peel strength. Epoxide modification of phenolic novolac resins will improve the peel strength by reducing shrinkage during cure, as well as improving chemical resistance, film strength, and adhesion.[4,5] Phenolic novolac resins, which under acidic conditions are the reaction products of formaldehyde and excess phenol, form repeating units such as shown in *Scheme* 1.[6,7] Due to high reactivity of hydroxyl functionalities, phenolic novolacs are easily modified with ECH in the presence of an alkali catalyst.[8,9]

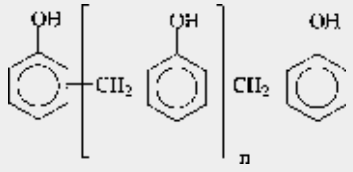

Scheme A

In order to cure epoxy resins as thermoset networks, it is necessary to use crosslinkers, such as amines, hydrazines, carboxylic acids, or anhydrides. The choice of a crosslinker will strongly influence mechanical properties and cure time of the final polymer network. In this study, the use of a phenolic novolac crosslinker will produce a hard, tough thermoset that exhibits excellent adhesion.[6] The mechanism of cure involves two etherfication reactions. The first is the reaction of a phenolic hydroxyl and epoxide to form an aromatic ether and 2° hydroxyl via a carbonium ion complex (*Scheme* 2A). The second involves the reaction of 2° hydroxyl groups and epoxide to form an aliphatic ether (*Scheme* 2B).[10,11] The second reaction depends on the concentra-

*Person to whom correspondence should be sent: The University of Southern Mississippi, Dept. of Polymers and High Performance Materials, Hattiesburg, MS 39406
†Studies conducted at North Dakota State University

tion of oxirane and the nature and concentration of catalyst. When 2-MI is used as a catalyst, the extent of reaction for secondary hydroxyl groups has been shown to vary from 50 to 90%.[12]

One of the advantages of using epoxy phenol novolac (EPN) resins is their ability to be formulated into powder coatings. In this study, we investigated how particle size of EPN powder coatings affects chemical reactivity at the film-substrate (F-S) interface and their adhesion. In an effort to understand the crosslinking reactions of EPN with phenol novolac resins, we utilized isothermal DSC measurements to monitor thermal kinetic behavior of EPN powder coatings and obtain activation energies of the crosslinking reactions. In an effort to understand molecular level processes as a function of particle size, time, and temperature leading to crosslinking reactions, attenuated total reflectance (ATR) Fourier transform infrared (FTIR) spectroscopy was used. In view of these considerations, we attempted to correlate these findings with pull-off adhesion measurements.

EXPERIMENTAL

Sample Preparation

Epoxy-modified phenol novolac powder coating samples with a well defined mean particle diameter of 21 ± 1 μm and 83 ± 1 μm were obtained from H.B. Fuller. This system is a two-component formulation which consists of the epoxy-modified phenol novolac and a phenolic crosslinking agent. To accelerate the crosslinking process, 2-methyl imidazole (2-MI) was added as a catalyst. Each particle size powder was applied to a 3 cm × 10 cm Al substrate using electrostatic spray (Nordson Versa-Spray II) at a 30 kV potential under operating pressures of 20 psi (atomizing), 30 psi (flow), and 3 psi (fluidizing). All specimens were crosslinked at 110, 140, and 170°C for 5, 10, 15, and 20 min. Crosslinked film thickness of 100-125 μm was determined using optical microscopy.

DSC Measurements

Differential scanning calorimeter (DSC) (Perkin-Elmer Model 7) was used to measure kinetics of the crosslinking reactions. Prior to analysis, temperature and calorimetric parameters were calibrated using indium. Dynamic DSC (DDSC) and isothermal DSC (IDSC) were performed on powder coatings sealed in an Al cell under an N_2 atmosphere (flow rate: 10 ml/min). The sample weight used in these experiments ranged from 9-14 mg. DDSC analysis was performed to determine the reaction exotherm and extent of crosslinking.[13] The average reaction heat was measured from DDSC traces using heating rates of 1, 5, 10, 15 and 20°C/min. For IDSC analysis, the sample was heated at 500°C/min to the isothermal temperature, after which data was collected until a stable baseline in the thermogram was achieved. Kinetic parameters were calculated using Perkin-Elmer 7 Series/UNIX isothermal kinetics software.[14,15]

Table 1—Dynamic Reaction Kinetics Parameters

Reaction System	Scan Rate (°C/min)	Q_T (mW)	Average Q_T (mW)
EPN 21 μm particle size	1	611	625
	5	613	
	10	618	
	15	639	
	20	644	
EPN 83 μm particle size	1	561	585
	5	581	
	10	589	
	15	594	
	20	601	

Spectroscopic Measurements

Attenuated total reflectance (ATR) FTIR spectroscopy was used to analyze the EPN specimens by observing the film-substrate (F-S) and film-air (F-A) interfaces. The spectra were collected on a Nicolet Magna 850 spectrometer, by co-adding 50 scans at a resolution of 4 cm^{-1}, Happ-Genzel apodization, and two levels of zero-filling. A variable angle ATR accessory equipped with a rectangular KRS-5 ATR crystal (Spectra Tech) was aligned to give an incident beam angle between 45 and 60°. Using a polarized filter, spectra were obtained with TM (0°) and TE (90°) polarizations to spectroscopically determine orientation of surface species. Calibration curve for oxirane band at 900 cm^{-1} was determined by monitoring IR intensity of a known concentration of biphenol-A and plotting it as a function of concentration. The spectra were corrected for optical effects using the Q-ATR algorithm with Grams/32 (Galactic Industries Corporation) software.[16]

Adhesion Measurements

Adhesion was measured using an Elcometer Model 106 adhesion tester (Elcometer Instruments, Ltd.). All powder coating specimens for adhesion analysis were electrostatically sprayed onto aluminum panels and crosslinked at temperatures of 110, 140, and 170°C for time intervals corresponding to the particular experiment. Al dollies were attached to the crosslinked films with a two-component epoxy adhesive (Araldite), and allowed to cure for 72 hr prior to dolly pull measurements.

RESULTS AND DISCUSSION

In order to elucidate the origin of crosslinking reactions of the polyfunctional epoxide and phenolic forming a crosslinked macromolecular structure, it is important to determine how particle size will affect kinetics of crosslinking reactions. For that reason, we compared reaction kinetics of 21 and 83 μm diameter powders to determine activation energies of the crosslinking reactions shown in *Scheme* 2. Ultimately, our goal is to determine the relationship between the particle size and adhesion of powder coatings. In a typical coalescence scenario for powders, the EPN powder is heated and powder particles will reach a molten state in a finite time period in which the reactions involved in the crosslinking

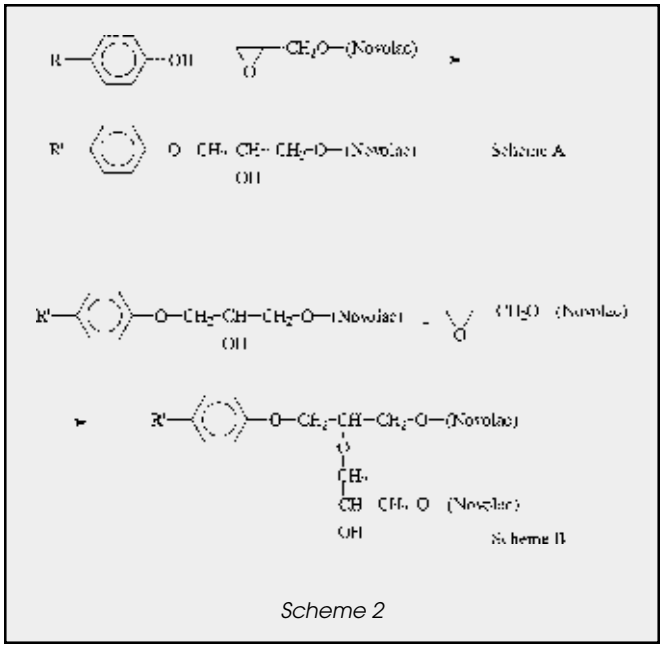

Scheme 2

process will occur. Since the ring-opening of the oxirane functionality is an exothermic reaction, it can be followed by DSC. Although both powder coatings have the same chemical makeup, the effect of particle size on the reaction kinetics may be affected by diffusion processes occurring at a given time and temperature.

Previous studies have examined kinetic behavior of epoxies using thermo-analytical measurements.[17,18] The basic assumption in DSC kinetics is that reaction rates are proportional to a heat flow, as denoted by the following equation:

$$\frac{d\alpha}{dt} = \frac{1}{Q_T} \times \frac{dq}{dt} \qquad (1)$$

where α is the fractional conversion of the reactants to products (for the extent of reaction), t is the reaction time (s), and Q_T is the total heat of reaction (mW). The rate of reaction, $d\alpha/dt$, is assumed to be the product of two functions, $\kappa(T)$ and $f(\alpha)$. While $\kappa(T)$ is defined by the Arrhenius equation, $f(\alpha)$ will be defined by the reaction rate. To describe an nth order reaction in terms of the extent of reaction, the kinetic equation is shown as:

$$\frac{d\alpha}{dt} = \kappa(1-\alpha)^n = \kappa \times f(\alpha) \qquad (2)$$

where κ is the reaction rate constant (s^{-1}), and n is the reaction order. By utilizing equations (1) and (2), the kinetic parameters can be obtained from isothermal DSC analysis at different temperatures. Fitting data from an isothermal curve for a given value of α, kinetic equations can be simplified to yield the reaction rate constant, κ. Using linear regression analysis of the rate constant data at each isothermal temperature, the activation energy (E_{act}) of this reaction can be determined.

In an effort to determine temperature ranges for isothermal measurements, DDSC was performed. As shown in *Figure* 1, scanning over the crosslinking temperature

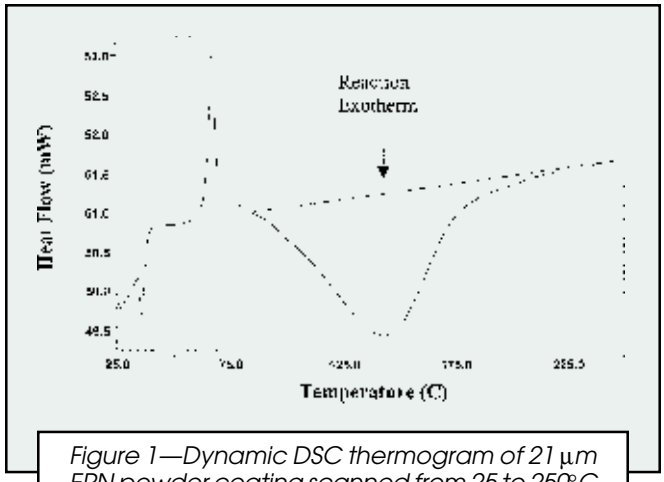

Figure 1—Dynamic DSC thermogram of 21 μm EPN powder coating scanned from 25 to 250°C at 10°C/min; reaction exotherm measured at 144°C.

range allows us to monitor the reaction exotherm. As can be seen from the thermogram, the onset of the reaction exotherm is at 80°C, which is the point at which the lowest isothermal measurement will be made. Subsequent isothermal measurements were made at equal intervals throughout the exotherm range. The reaction heat (Q_T) measured from DDSC traces is shown in *Table* 1, from which the average Q_T is calculated.

In isothermal analysis, the DSC curve shape is indicative of the kinetics, and in the isothermal trace shown in *Figure* 2, an immediate exothermic peak is followed by exponential decay, which is characteristic of an nth order kinetics model. Using these data, an extent of cure (α) as a function of isothermal reaction temperature was determined using equations (1) and (2). This is shown in *Figure* 3, and it appears that a 21 μm particle diameter powder system exhibits a higher extent of reaction at temperatures up to 155°C, as compared to that of the 83 μm diameter. As the temperature increases above 155°C, the extent of crosslinking difference between the two particle sizes narrows, and at 185°C, the extent of crosslinking between the two powder coatings is similar. Based on these data, it is apparent that the delayed

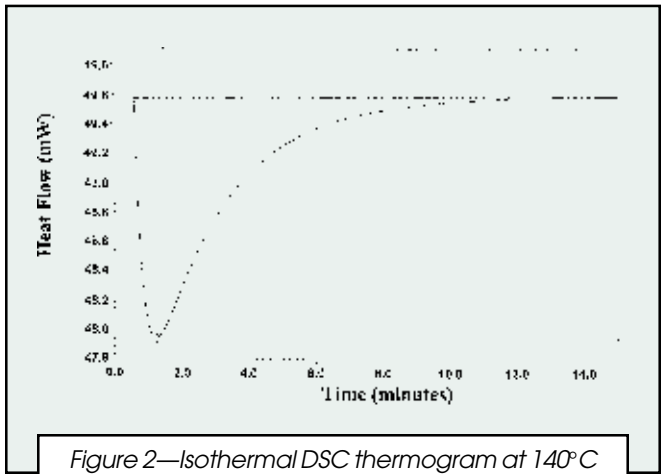

Figure 2—Isothermal DSC thermogram at 140°C for 21 μm EPN powder coatings; reaction exotherm measured at 1.2 min.

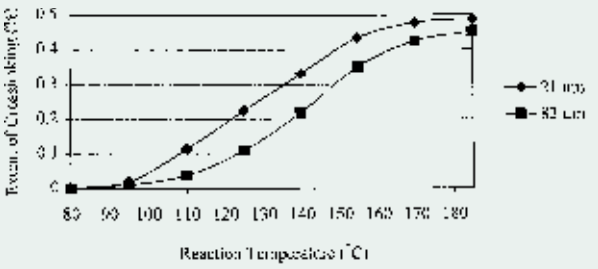

Figure 3—Extent of crosslinking for 21 and 83 μm particle size powder coatings as a function of reaction temperature.

increase in the coarser particle reaction is due to the difference in particle size.

If one assumes that crosslinking kinetics at various temperatures obey Arrhenius behavior, the following relationship can be applied:

$$\ln(\kappa) = \ln(A) - E_{act}/RT \quad (3)$$

where A is the frequency factor (s^{-1}), R is the gas constant (8.31 J $mol^{-1}K^{-1}$), T is the temperature (K), and E_{act} (kJ/mol) is the activation energy. The thermal response data can be fitted to equations (1) and (2) to derive the crosslinking reaction rate constant, κ. In *Figure* 4, ln (κ) is plotted as a function of 1/T which will allow us to obtain activation energies (E_{act}) for 21 and 83 μm particle size powder systems. From the slopes shown in *Figure* 4, the E_{act} values of 41 kJ/mol for the 21 μm powder and 58 kJ/mol for the 83 μm powder are determined. The E_{act} data, as well as the frequency factor, ln (A), and reaction order, n, are summarized in *Table* 2.

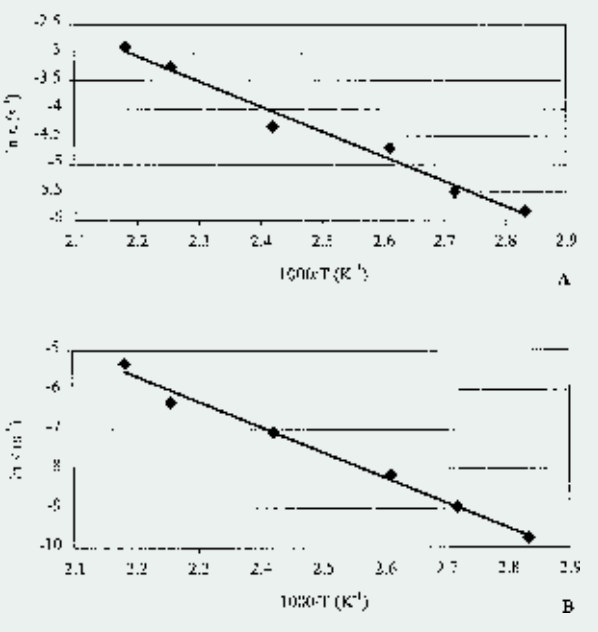

Figure 4—Arrhenius plots for (A) 21 μm particle diameter EPN powder coating and (B) 83 μm particle diameter EPN powder coating.

Based on the previous data, if the crosslinking reactions are solely controlled by the kinetics of chemical reactions, the E_{act} values for the 21 and 83 μm diameter powder coatings should be the same. In view of the differences of the activation energies, two questions need to be addressed: why activation energies are different and, what processes, other than kinetics, control crosslinking behavior? Before we address these issues, let us consider differences between the particle kinetic data which suggest that activation energies are intrinsically related to the film formation process. In order for crosslinking reactions to occur, reacting functional groups must be in a close proximity to each other. Because diffusion of polymer chains depends on viscosity, particles converted to a molten, lower viscosity state react faster. Thus, it is appropriate to consider thermal conductivity and its effect on melting behavior of both diameter powder particles.

Several studies have shown the dependence of reaction rates in thermally crosslinked systems with the increase of molecular weight, which directly involves a change in melt viscosity.[19,20] In the reactions shown in *Scheme* 2, the rate of crosslinking is kinetically controlled, up to the point of vitrification.[21] At the onset of melting, the extent of crosslinking and the melt viscosity are low. As reactions continue, the coating will form a stable interface with the substrate as the adhesive interphase forms. In order to understand the crosslinking behavior of EPN powders, let us consider the effect of particle size on the melting point. Observation of the melt behavior of powders as a function of temperature shows that powder packing plays a key role in which the melting point of a specimen will depend on the thermal conductivity of the heated surface. Since the thermal conductivity coefficient of air is much lower than that of organic polymers, the presence of voids will extend the time required for a specimen to melt due to lower contact area between neighboring particles. In the case of EPN powders, thermal conductivity of a 21 μm particle size will be approximately four times greater than an 83 μm particle.[22] Therefore, smaller particle size powders will be expected to reach a molten state in 25% shorter times than larger sizes. Therefore, extent of crosslinking reactions at a given temperature will be greater for smaller particles. As the temperature increases, the magnitude of thermal transfer will also increase, and thus, extent of reactions for larger particle sizes will be similar to those with a smaller particle size. In essence, a combination of time-temperature-particle size transition will determine the extent of crosslinking.

Although thermal analytical techniques are useful in determining thermal behavior of polymers, they are insufficient when quantitative analysis of crosslinking groups is desired. The degree of crosslinking in EPN powder coatings can be determined spectroscopically

Table 2—Isothermal Reaction Kinetics Parameters

Reaction System	ln A (s^{-1})	n	E_{act} (kJ/mol)
EPN 21 μm particle size	6.84	2	41
EPN 83 μm particle size	8.47	2	58

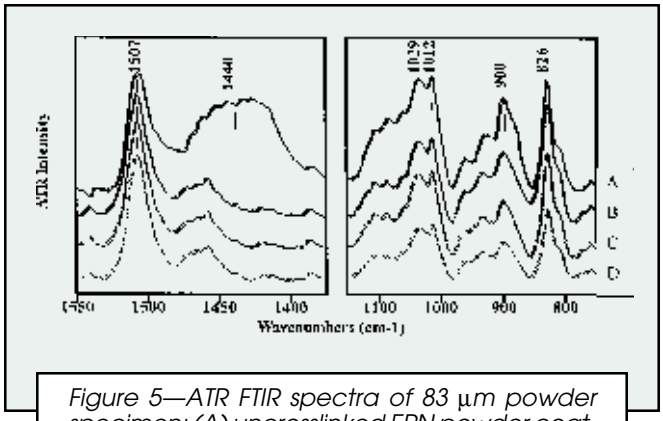

Figure 5—ATR FTIR spectra of 83 μm powder specimen: (A) uncrosslinked EPN powder coating, (B) EPN powder coating crosslinked at 110°C for 10 min; (C) EPN powder coating crosslinked at 110°C for 30 min; and (D) EPN powder coating crosslinked at 110°C for 60 min.

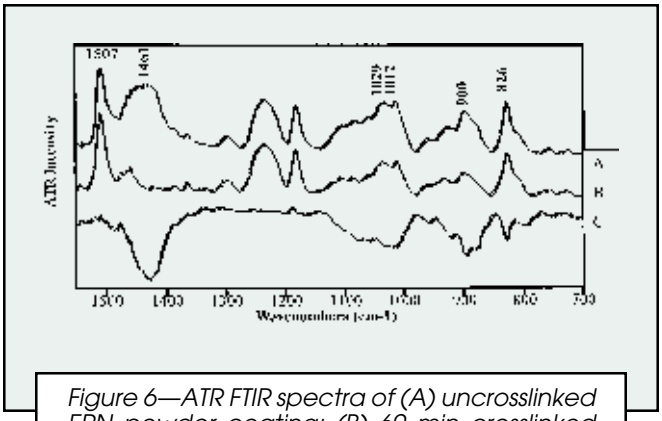

Figure 6—ATR FTIR spectra of (A) uncrosslinked EPN powder coating; (B) 60 min crosslinked EPN powder coating; and (c) subtracted spectra, A—B.

by monitoring oxirane and hydroxyl functionalities. However, our particular interest was reactions occurring near the F-S interface because this interface is ultimately responsible for adhesion. For that reason, we utilized ATR FTIR spectroscopy.

Figure 5 illustrates ATR FTIR spectra of 83 μm particle size epoxy-modified phenol novolac powder coating films at various stages of crosslinking. Traces A-D illustrate the spectra recorded at the F-S interface of 83 μm particle powder crosslinked at 110°C for 0 to 60 min. As a first step in spectroscopic analysis, it is necessary to establish the origin of infrared bands. As a means to interpret bands involved in crosslinking reactions at various stages of crosslinking, *Table* 3 lists the observed bands and their tentative assignments.[23-25] As seen in *Figure* 5, it is apparent that the bands at 1012 and 900 cm^{-1} due to the asymmetric and symmetric C–O–C stretching modes of oxirane decrease with increasing crosslinked time. The bands at 1029 and 826 cm^{-1} due to the O–H and C–O groups of the phenolic crosslinker also exhibit lower intensity at extended crosslinking times. The 1461 cm^{-1} normal vibrations of phenolic hydroxyl groups and detected 1440 cm^{-1} band due to hydrogen bonding, also decrease. The band at 1507 cm^{-1} is due to the benzene ring and therefore, independent of the degree of cure, but proportional to the amount of the coating. Since this band remains constant at all stages of cure, it will be used as an internal reference standard in these studies.[26] To further define the functional groups involved in the crosslinking process, *Figure* 6 illustrates the difference spectrum of an 83 μm EPN film crosslinked at 110°C for 60 min, subtracted from an uncrosslinked 83

Table 3—Tentative Infrared Band Assigments for Uncured Epoxy-Modified Phenol Novolac Powder Coating

Wavenumber (cm^{-1})	Band Assignment	Component
3493	ν(OH)	PN
3053	$\nu_{as}(CH_2)$	EPN
1608	ν(C=C) φ	PN
1583	ν(C=C) φ	PN
1507	ν(C=C) φ + ν (N=C–N)	PN
1461	δ(OH) + ν (C–O)	PN
1440	H-bonded δ (OH)	PN
1295	ν(C–C) + ν (C–O)	PN
1233	ν(C–O) + δ (φ–H) in-plane	PN
1181	δ(φ–H) in-plane	PN
1066	ν_{as}(φ–O–C)	PN
1029	ν(φ–O–H)	PN
1012	ν_{as}(C–O–C)	EPN
936	δ(φ–H) out-of-plane	PN
900	ν_{s}(C–O–C)	EPN
826	ν(C–O) + ν (O–H) in-plane and out-of-plane	PN
770	δ(φ–H) out-of-plane	PN
755	ω(CH_2)	EPN
641	δ(C-OH) out-of-plane	PN

ν: stretching
δ: deformation
ω: wagging
φ: aromatic ring
PN: phenolic novolac
EPN: epoxy-modified phenolic novolac
2-MI: 2-methyl imidazole (catalyst)

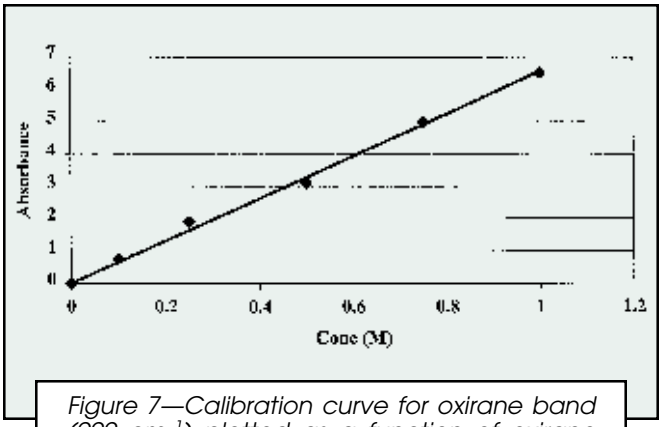

Figure 7—Calibration curve for oxirane band (900 cm^{-1}) plotted as a function of oxirane concentration.

μm specimen. The criterion for subtraction is elimination of the 1507 cm^{-1} normalization band. The major features of the difference spectrum are observed at 1461, 1029, and 826 cm^{-1} due to the phenolic resin participation in the crosslinking reactions, as well as the 1012 and 900 cm^{-1} band responsible for oxirane group consumption. This analysis shows that band intensities of the difference spectra due to phenol groups diminishes their intensity at a higher rate than that due to epoxy. This discrepancy comes from the fact that phenol groups are consumed in reactions not resulting from the crosslinking with epoxy; instead condensation of the hydroxyl groups in the presence of a catalyst may occur. It should be noted that 21 and 83 μm particle size powders exhibit the same chemical composition prior to crosslinking reactions, thus any spectroscopic changes observed in the spectra result from crosslinking reactions.

In an effort to relate oxirane consumption to adhesion, let us quantify oxirane concentration. Using quantitative procedures outlined in the previous studies,[26,27] analysis of the decrease in oxirane concentration as a function of crosslinking time is made. ATR FTIR spectroscopy is used to monitor the intensity of the oxirane bands at 900 cm^{-1} due to oxirane breathing vibrations.[28] Because quantitative use of ATR FTIR spectroscopy requires a calibration curve, *Figure* 7 was constructed, plotting known concentrations of oxirane as a function of the 900 cm^{-1} band intensity.[29,30] Using Beer-Lambert's Law, one can determine a molar absorption coefficient of oxirane from the slope of the calibration curve which is equal to 528.7 L/mol·cm, followed by quantitative assessment using Q-ATR of the oxirane concentration at various crosslinking times.[16]

When oxirane concentration is plotted as a function of the reaction time for a given temperature, oxirane concentration decreases. This is illustrated in *Figure* 8 which shows decreasing oxirane concentration for the 21 and 83 μm powder systems at increased reaction times and temperatures. Quantitative analysis of the F-S interface shows a change in oxirane concentration from 5.87×10^{-3} M to 2.11×10^{-3} M for the 21 μm particle size upon crosslinking at 185°C for 20 min. Likewise, for the 83 μm particle under the same conditions, the oxirane concentration decreases from an uncrosslinked concentration of 5.02×10^{-3} M to 2.63×10^{-3} M. Thus, the oxirane functionality decreases at a faster rate for smaller particle sizes, with the differences more apparent at intermediate temperatures and reaction times.

As a means to determine differences in reactivity as a result of the surrounding environment, powder coating films were analyzed using ATR spectroscopy at the F-A and F-S interfaces. A spectral comparison between the interfaces show virtually no variation in the 900 cm^{-1} band for the 21 μm particle size. For the 83 μm particle, slightly higher oxirane concentration (10^{-5} M difference) is observed at the F-A, suggesting that the thermal and chemical conditions encountered at the F-A and F-S are similar for the 21 μm particle size powder system, but other factors may influence crosslinking reactions of the 83 μm coating. In addition, depth profiling studies of the powder coatings revealed that no crosslinking stratification is observed from 0 to 2 μm below the surface. Since adhesive interactions will be localized at the coating-substrate interface, the remainder of this study will focus on the analysis of the F-S interface.

Spectroscopic determination of the orientation of surface species is accomplished by the use of polarized light.[25] The polarized ATR FTIR spectra of 21 and 83 μm EPN powder coating indicate that the oxirane and the hydroxyl functionalities have no preferred surface orientation near the F-S interface. Therefore, the particle

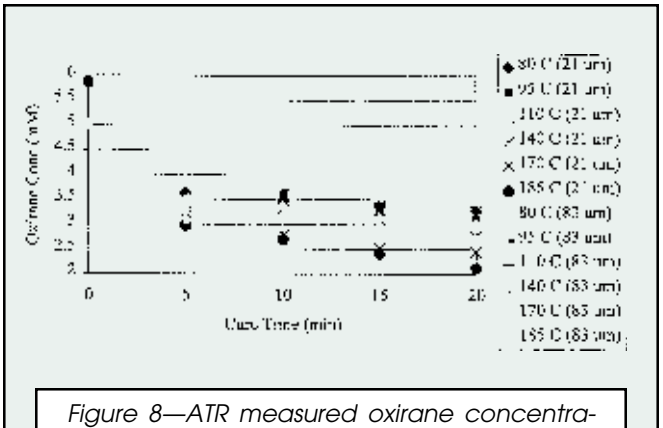

Figure 8—ATR measured oxirane concentration (mM) plotted as a function of crosslinking time under isothermal conditions.

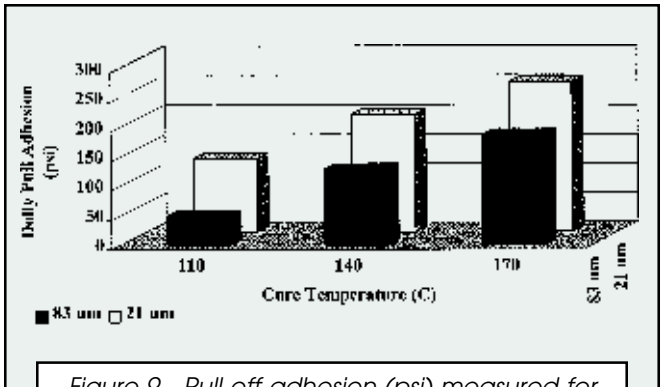

Figure 9—Pull-off adhesion (psi) measured for powder coating on Al substrate for 21 and 83 μm particle powder films crosslinked at 110, 140, and 170°C for 10 min.

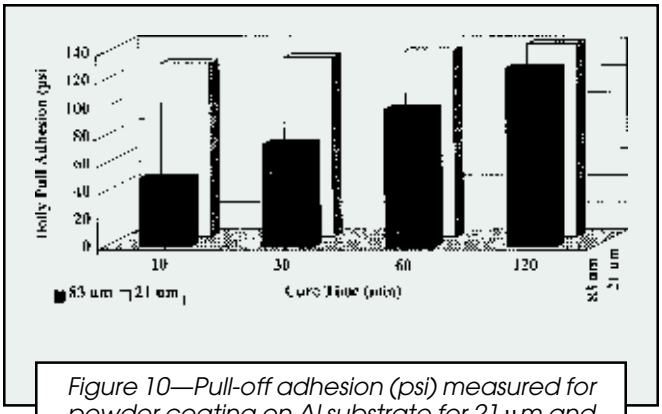

Figure 10—Pull-off adhesion (psi) measured for powder coating on Al substrate for 21 μm and 83 μm particle powder films crosslinked at 110°C for 10, 30, 60, and 120 min.

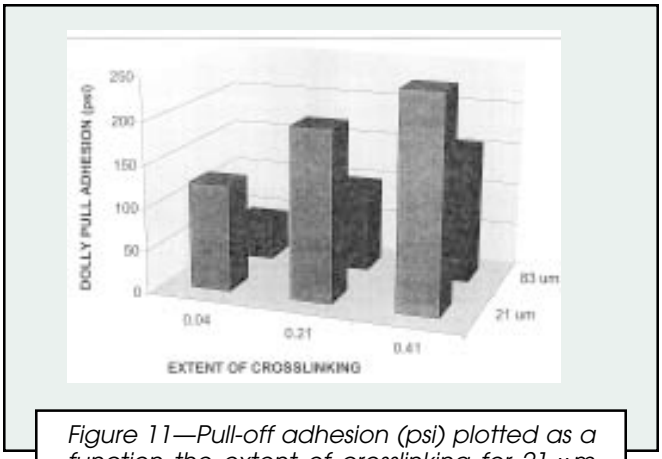

Figure 11—Pull-off adhesion (psi) plotted as a function the extent of crosslinking for 21 μm and 83 μm particle powder films crosslinked at 110, 140, and 170°C for 10 min.

size does not appear to play a role in the orientation of these groups. This behavior is expected since the chemical composition of each particle size is the same, and the diameter of the particle has no influence on the oxirane group orientation.

Although there are numerous sources that may contribute to improvement of adhesion, it is known that a smaller particle size will have more efficient packing, less void space, and therefore, may exhibit enhanced adhesion due to the greater number of surface functionalities present at the F-S interface. Increased surface area allows for increased functional group interactions which leads to a higher reaction efficiency.[31] An important factor to consider is improved wetting during the crosslinking stages which, for the smaller chemical powder makeup, would be enhanced for smaller particle powders due to higher thermal conductivity, increased particle-particle contact, and a lower viscosity, resulting in improved penetration into the substrate. As shown in the previous studies,[22] finer powder particles exhibit improved flow properties and the time (t) required for a powder particle to completely coalesce into a continuous film is shown by:

$$t = \frac{\chi \eta r}{\gamma} \qquad (4)$$

where χ is a constant, η is the viscosity of the powder coating, r is the radius of the powder particle, and γ is the surface tension of the coating.[4,22]

Due to oxirane concentrations measured at the particle surface and particle size effect on surface area and packing efficiency, let us examine how adhesion varies with the particle size for a given time-temperature-particle size-transition. Adhesion measurements for both particle sizes crosslinked at 110, 140, and 170°C for 10 min are illustrated in *Figure* 9. These results indicate that consistently higher adhesion occurs at all crosslinking temperatures for the 21 μm particle size. Correlation of the data obtained from DSC and ATR measurements indicates that a significantly higher extent of crosslinking would be expected for the 21 μm particle coating under these conditions. Since the reactions involved in the crosslinking process will also contribute to chemical and mechanical interactions, enhanced adhesion would be expected. The thermal lag associated with larger particle size may also reflect the lower adhesive values for the 83 μm film, as the film fails to properly wet the substrate. These observations are reflected in the difference in the activation energies, in which 21 μm is lower than 83 μm diameter particles. It should be noted that these results also indicate an obvious connection between the effect of particle size on the production throughput and economics of the process.

Figure 10 further defines the relationship between powder coating melt behavior and adhesion for extended cure times at 110°C. This experiment shows that the two particle sizes will approach similar adhesion performance, given the required time for crosslinking. As cure time increases from 10 min to 120 min, adhesion of the 83 μm powder improves dramatically, while the 21 μm powder improves at a comparatively slower rate. As was shown in *Figure* 8, the reaction of oxirane functionalities at 10 min is more pronounced for the 21 μm particle size when compared to 83 μm, but similar oxirane concentrations are observed at extended time periods. These results clearly show that the extent of crosslinking in powder coatings, which for liquid coatings would be adequately described by time-temperature-transition (TTT),[32] is affected by a particle size, and for that reason time-temperature-particle size (TTPS) transformation reflects processes in crosslinking of powders. As shown in *Figure* 10, overcoming the lower thermal conductivity inherent to the larger particle sizes, crosslinking of both powders are found to be nearly identical, which is reflected in a correlation between the extent of crosslinking and adhesion as a function of temperature. Although these data were indirectly presented in *Figures* 3, 9, and 10, *Figure* 11 was constructed to illustrate that for 21 μm particle size the highest crosslinking enhances adhesion.

CONCLUSIONS

These studies show that the effect of particle size may significantly influence the crosslinking kinetics as well as adhesion of powder coatings to metal substrates. En-

hancement of pull-off adhesion for the 21 μm particle size crosslinked is attributed to time-temperature-particle size transition, and it appears that smaller particle sizes exhibit higher adhesion. The effect of particle size is attributed to the higher thermal conductivity of the finer powders, resulting in improved wetting of the substrate in a molten state, thus promoting chemical and mechanical adhesion. Smaller particles provide shorter cure times, thus powder coalescence plays a very important role in achieving crosslinking and proficient adhesion.

ACKNOWLEDGMENTS

The authors are thankful to Wayne Eklund, Industrial Coatings Division of H.B. Fuller Company, Vadnais Heights, MN for the preparation of powder coatings. A partial financial support is acknowledged from the Powder Coatings Institute, the National Science Foundation Industry/University Cooperative Research Center in Coatings at North Dakota State University, and Eastern Michigan University.

References

(1) Tess, R.W. and Poehlein, G.W., *Appl. Polymer Sci.*, American Chemical Society, Washington, D.C., 1985.
(2) Paul, S., *Surface Coatings: Science and Technology*, Wiley, Chichester, 1985.
(3) Wicks, Z., Jones, F., and Pappas, S., *Organic Coatings: Science and Technology*, Vol. 1, Wiley, New York, 1992.
(4) Misev, T.A., *Powder Coatings: Chemistry and Technology*, Wiley, Chichester, 1991.
(5) Odian, G., *Principles of Polymerization*, Wiley, New York, 1991.
(6) Knop, A. and Pilato, L.A., *Phenolic Resins: Chemistry, Applications, and Performance*, Springer-Verlag, Berlin, 1985.
(7) Ulrich, H., *Introduction of Industrial Polymers*, Hanser, New York, 1993.
(8) Greenspan, F.P., in *Chemical Reactions of Polymers*, Fettes, E.M. (Ed.), Interscience, New York, 152, 1964.
(9) *Chemistry and Technology of Epoxy Resins*, Ellis, B. (Ed.), Blackie, Glasgow, 1993.
(10) Ishida, H. and Smith, M.E., *Polymer Eng. Sci.*, 32, 136 (1992).
(11) Bate, D.A., *The Science of Powder Coatings*, Vol. 1, Sita, London, 1990.
(12) Hsieh, T.H. and Su, A.C., *J. Appl. Polymer Sci.*, 44, 165 (1992).
(13) Flynn, J.H., *J. Thermal Analysis*, 37, 293 (1991).
(14) Gray, A.P., *Proc. American Chemical Society Symposium, Analytical Calorimetry*, 209, 1968.
(15) Freeman, E.S. and Caroll, B., *J. Phys. Chem.*, 62, 394 (1958).
(16) Urban, M.W., *ATR Spectroscopy of Polymers: Theory and Practice*, American Chemical Society, Washington, D.C., 1996.
(17) Gordon, M. and Scantlebury, G.R., *Trans. Faraday Soc.*, 60, 605 (1964).
(18) Dusek, K., Ilavsky, M., and Matejka, L., *Polymer Bull.*, 12, 33 (1984).
(19) Flory, P.J., *Macromolecules*, 15, 99 (1982).
(20) Allen, G., Booth, C., and Price, C., *Polymer*, 8, 397 (1967).
(21) Eyring, H., Lin, S.H., and Lin, S.M., *Basic Chemical Kinetics*, Wiley, New York, 1980.
(22) Nix, V.G. and Dodge, J.S., "Rheology of Powder Coatings," JOURNAL OF PAINT TECHNOLOGY, *45*, No. 586, 59 (1973).
(23) Socrates, G., *Infrared Characteristic Group Frequencies*, Wiley, New York, 1980.
(24) Colthup, N., Wiberley, S., and Daly, L., *Introduction to Infrared and Raman Spectroscopy*, Academic Press, San Diego, CA, 1990.
(25) Urban, M.W., *Vibrational Spectroscopy of Molecules on Surfaces*, Wiley, New York, 1993.
(26) Mertzel, E. and Koenig, J.L., in *Epoxy Resins and Composites II, Advances in Polymer Science*, Vol. 75, Dusek, E. (Ed.), Springer-Verlag, Berlin, 1986.
(27) Huang, J.B. and Urban, M.W., *Appl. Spectrosc.*, 46, 1014 (1992).
(28) Huang, J.B. and Urban, M.W., *Appl. Spectrosc*, 46, 1666 (1992).
(29) Kaminski, A.M. and Urban, M.W., "Interfacial Studies of Crosslinked Polyurethanes: Part I. Quantitative and Structural Aspects of Crosslinking Near Film-Air and Film-Substrate Interfaces in Solvent-Borne Polyurethanes," JOURNAL OF COATINGS TECHNOLOGY, *69*, No. 872, 55 (1997).
(30) Kaminski, A.M. and Urban, M.W., "Interfacial Studies of Crosslinked Urethanes: Part II. The Effect of Humidity on Waterborne Polyurethanes; A Spectroscopic Study," JOURNAL OF COATINGS TECHNOLOGY, *69*, No. 873, 113 (1997).
(31) Podczeck, F., *J. Adhes. Sci. Technol.*, 11, 1089 (1997).
(32) Wisanrakkit, G. and Gillham, J.K., *Advances in Chemistry Series 227*, Craver, C.D. and Provder, T. (Eds.), American Chemical Society, Washington, D.C., 1990.